Pergamon

Int. J. Solids Structures Vol. 33, No. 14, pp. 2075–2093, 1996

0020-7683/96 $15.00 + .00

0020-7683(95)00144-1

AN ANALYTICAL APPROACH TO THE STRESS FIELD IN THE EXTRUSION OF BIMETALLIC TUBES

J. L. ALCARAZ and J. M. MARTÍNEZ-ESNAOLA
Departamento de Ingeniería Mecánica-Escuela Técnica Superior de Ingenieros Alameda Urquijo, s/n-48013 Bilbao, Spain

and

J. GIL-SEVILLANO
Centro de Estudios e Investigaciones Técnicas de Guipúzcoa (CEIT) and Escuela Superior de Ingenieros Industriales (Universidad de Navarra)-P° Manuel de Lardizábal, 15-20009 San Sebastián, Spain

(*Received* 21 *October* 1994; *in revised form* 16 *June* 1995)

Abstract—In this paper an analytical solution for the extrusion of bimetallic tubes is deduced by assuming an axially-symmetric radial flow through a conical die. Different extrusion conditions and different material combinations are considered to assess the stress levels at critical zones. Solutions for the two possible locations of the harder material (acting as an inner or outer lining) are presented. The analysis highlights the effects on the extrusion process of a number of parameters, such as the yield stress ratio between the materials, the die angle and the volume fraction of the harder component. A ductile failure factor is introduced and evaluated for all the cases contemplated in the paper.

1. INTRODUCTION

Bimetallic combinations are increasingly present in many different industrial applications. Here we are concerned with bimetallic tubes, used, for example, for oil conductions in sour wells. In this mentioned application, as in many others, a good corrosion resistance, as well as a high mechanical strength, are required. Under these conditions, a bimetallic combination proves to be more economical than a nonmetallic tube of a corrosion resistant alloy.

Mostly, bimetallic tubes are produced by the well-known extrusion process. Much work has been devoted to the stress analysis of this process. One of the pioneering works is the analysis of Shield (1955), who considered the radial flow of a single material through conical dies, and proposed a numerical resolution for the equations governing the stress field. With the same type of analysis, Blazynski and Townley (1978) analysed the process of plug drawing of bimetallic tubing in implosively welded composites under plane strain conditions. A mean strain hardening is also included. More recently, Durban (1984) found a complete analytical solution following a Shield-type analysis and assuming small extrusion die angles. Durban also applied the results to a multilayered composite in drawing and extrusion operations.

A different type of analysis is that of Atkins and Weinstein (1970), who applied the force equilibrium approach to a bimetallic rod, assuming a rigid-plastic constitutive model. Later, Blazynski and Townley (1978) extended the analysis of Atkins and Weinstein to strain-hardening conditions.

Other analyses (Blazynski and Townley, 1978; Hartley, 1973; Tokuno and Ikeda, 1991; Taheri, 1993; Yang *et al.*, 1991) use the upper bound approach to determine the power required for the process. Moreover, the upper bound method has been used by others to introduce a failure condition in the bimetallic flow (Avitzur, 1982, 1986; Osakada *et al.*, 1973; Nagy, 1985). The method, however, does not concentrate on the stress field within the working zone.

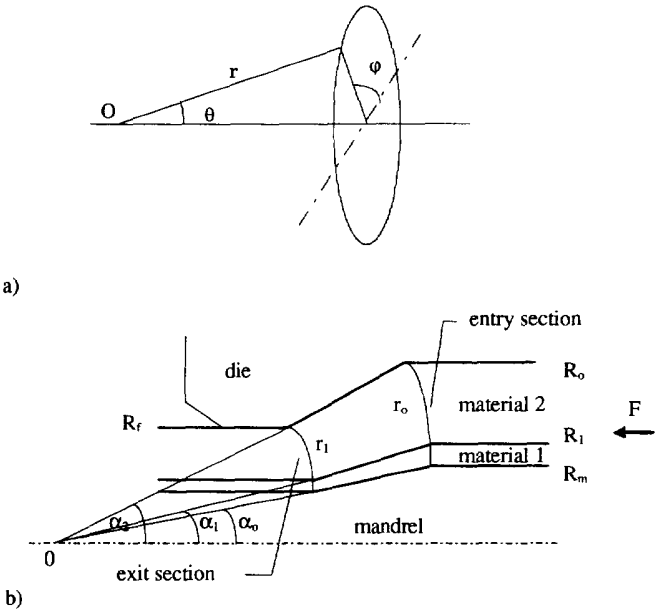

Fig. 1. (a) Spherical coordinates used in the analysis, (b) geometry of the process.

In this paper, we seek for the stress determination during the flow of a bimetallic tube through a conical die. One of the two materials (the thinner layer) is referred to as the corrosion resistant alloy and the other as the base steel. The analysis follows the initial steps of Durban's, but provides a more general solution valid for any die angles, and illustrates the influence of the different extrusion parameters on the stress field.

2. AXISYMMETRIC STRESS FIELD FOR A FLOWING MATERIAL

Our aim in this section is to find a general expression for the stress field of a single material flowing radially with axial symmetry. Spherical coordinates (r, θ, φ) with origin in O are used, as shown in Fig. 1a.

With the assumption of an axially-symmetric radial flow, the application of the condition of material incompressibility leads to the following velocity field:

$$u = -\frac{f(\theta)}{r^2} \quad (v = w = 0) \tag{1}$$

where u stands for the radial velocity; v, w are the other two components, and $f(\theta)$ is an unknown function of the angular coordinate. The non-vanishing strain rate components, D_{ij}, easily deduced from (1), are $D_r = 2f/r^3$, $D_\theta = D_\varphi = -f/r^3$, $D_{r\theta} = -f'/2r^3$.

The isotropic flow imposes that $\sigma_\varphi = \sigma_\theta$ and the axial symmetry implies $\tau_{r\varphi} = \tau_{\varphi\theta} = 0$. Accordingly, von Mises yield condition for a rigid-perfectly plastic behaviour leads to:

$$(\sigma_r - \sigma_\theta)^2 + 3\tau_{r\theta}^2 = Y^2 \tag{2}$$

where Y denotes the yield equivalent stress. Besides, the equations of the isotropic plastic flow provide:

$$\frac{\tau_{r\theta}}{\sigma_r - \sigma_\theta} = \frac{D_{r\theta}}{D_r - D_\theta} = \frac{-f'(\theta)}{6f(\theta)} \tag{3}$$

Equation (2) can be written parametrically as:

$$\sigma_r - \sigma_\theta = Y\cos 2\Psi$$

$$\tau_{r\theta} = \frac{Y}{\sqrt{3}}\sin 2\Psi \tag{4}$$

where Ψ is a parameter (dependent on θ) that will be determined later.

By the radial and normal equilibrium equations, the following expressions are deduced (Shield, 1955):

$$2(\Psi' + \sqrt{3})\cos 2\Psi + \cot\theta \sin 2\Psi = \frac{2B\sqrt{3}}{Y} \tag{5}$$

$$(F - \sqrt{3}\cos 2\Psi)' + 3\sin 2\Psi = 0 \tag{6}$$

where B is an integration constant, and Ψ, F are still unknown functions of θ. Moreover, the radial stress is expressed by:

$$\sigma_r = -2B\ln r + \frac{Y}{\sqrt{3}}F(\theta) \tag{7}$$

Now, it is convenient to define the local friction factor m as

$$m = \frac{\sqrt{3}|\tau_{r\theta}|}{Y} = |\sin 2\Psi| \tag{8}$$

according to the second equation in (4). In nearly uniform flow patterns, friction stresses are relatively small compared to the yield stress (i.e., $|\tau_{r\theta}| \ll Y$). Therefore, $|\Psi|$ becomes much smaller than unity. The integration of Eqs (5) and (6) with this approach gives rise to the following expression for Ψ:

$$\Psi = \sqrt{3}\left(\frac{B}{Y} - 1\right)\tan\frac{\theta}{2} - \frac{\sqrt{3}K}{2Y\sin\theta} \tag{9}$$

where K is an integration constant. Equation (9) coincides with that obtained by Durban (1984), who proceeds the analysis by assuming small die angles. Here no restrictions on the die angle are imposed.

From (6) and (9), and applying $|\Psi| \ll 1$, it is obtained:

$$F' = -6\Psi = -6\sqrt{3}\left[\left(\frac{B}{Y} - 1\right)\tan\frac{\theta}{2} - \frac{K}{2Y\sin\theta}\right] \tag{10}$$

Integrating (10), the following expression is derived:

$$F = -6\sqrt{3}\left[-2\left(\frac{B}{Y} - 1\right)\ln\cos\frac{\theta}{2} - \frac{K}{2Y}\ln\tan\frac{\theta}{2}\right] + A\frac{\sqrt{3}}{Y} \tag{11}$$

where A is a constant. Therefore, according to (7), (4), (11) and (9), the stress field is given by:

$$\sigma_r = -2B\ln r + \frac{Y}{\sqrt{3}}F = A - 2B\ln r + 12(B-Y)\ln\cos\frac{\theta}{2} + 3K\ln\tan\frac{\theta}{2} \tag{12a}$$

$$\sigma_\theta = \sigma_r - Y\cos 2\Psi \approx \sigma_r - Y \tag{12b}$$

$$\tau_{r\theta} = \frac{Y\sin 2\Psi}{\sqrt{3}} \approx \frac{2Y}{\sqrt{3}}\Psi = 2(B-Y)\tan\frac{\theta}{2} - \frac{K}{\sin\theta}. \tag{12c}$$

The associated velocity profile is determined by (1), where $f(\theta)$ is a function satisfying:

$$\frac{\sqrt{3}}{6}\frac{f'}{f} = -2\sqrt{3}\left[\left(\frac{B}{Y}-1\right)\tan\frac{\theta}{2} - \frac{K}{2Y\sin\theta}\right]. \tag{13}$$

After integrating (13), we obtain:

$$f = C_0\exp\left[24\left(\frac{B}{Y}-1\right)\ln\cos\frac{\theta}{2} + \frac{6K}{Y}\ln\tan\frac{\theta}{2}\right] = C_0\left[\left(\cos\frac{\theta}{2}\right)^{24\left(\frac{B}{Y}-1\right)}\left(\tan\frac{\theta}{2}\right)^{\frac{6K}{Y}}\right] \tag{14}$$

where C_0 is a constant.

Having obtained the stress field and the velocity profile, only constants remain to be determined in (12) and (14) by applying the corresponding boundary conditions.

3. SOLUTION FOR A BIMETALLIC TUBE

The stress field derived in the above section will be used for the stress determination in the bimetallic combination. This implies that the flow is spherical and perfectly radial. Consequently, no velocity discontinuity can arise along the material interface. This is evidently an ideal case, not always attainable in real extrusions where the material heterogeneity is likely to prevent a perfectly compatible flow.

Figure 1b shows the geometry of the process. A tube composed of two materials is forced against a rigid conical die flowing over a fixed mandrel. In the notation that follows, subscript 1 will refer to the inner material and subscript 2 to the outer one. Moreover, the thinner layer corresponds to the corrosion resistant alloy and the other to the low-alloyed or base steel.

To obtain the stress solution in the bimetallic tube, the different contants in eqn (12) for each material are to be determined. In other words, we must impose the continuity and boundary conditions.

Firstly, across the material interface the normal and shear stresses are continuous. Using (12a), the continuity of the normal stress leads to:

$$-2B_1\ln r + A_1 + 12(B_1 - Y_1)\ln\cos\frac{\alpha_1}{2} + 3K_1\ln\tan\frac{\alpha_1}{2} - Y_1 =$$

$$-2B_2\ln r + A_2 + 12(B_2 - Y_2)\ln\cos\frac{\alpha_1}{2} + 3K_2\ln\tan\frac{\alpha_1}{2} - Y_2 \tag{15}$$

and through (12c) the continuity of the shear stress provides:

$$2(B_1 - Y_1)\tan\frac{\alpha_1}{2} - \frac{K_1}{\sin\alpha_1} = 2(B_2 - Y_2)\tan\frac{\alpha_1}{2} - \frac{K_2}{\sin\alpha_1}. \tag{16}$$

It is interesting to note that eqn (15) implies that $B_1 = B_2 = B$.

Secondly, as two boundary conditions, friction between the tube and the mandrel and the die is considered. By assuming the friction model given by (8) and constant friction coefficients, m_0 with the mandrel (at $\theta = \alpha_0$) and m_2 with the die (at $\theta = \alpha_2$), the following two equations are obtained:

$$2(B_1 - Y_1)\tan\frac{\alpha_0}{2} - \frac{K_1}{\sin\alpha_0} = -\frac{m_0 Y_1}{\sqrt{3}} \tag{17}$$

$$2(B_2 - Y_2)\tan\frac{\alpha_2}{2} - \frac{K_2}{\sin\alpha_2} = \frac{m_2 Y_2}{\sqrt{3}}. \tag{18}$$

Note that the friction with the mandrel provides a negative shear stress. Accordingly, there appears a minus sign in (17).

Finally, on the basis of a pure extrusion process, the axial component of the total force at the die exit should vanish. Using this boundary condition, the following expression is obtained:

$$\begin{aligned}
0 &= \int_{\alpha_0}^{\alpha_1} \sigma_r^{(1)}|_{r_1} \cos\theta \sin\theta \,\mathrm{d}\theta + \int_{\alpha_1}^{\alpha_2} \sigma_r^{(2)}|_{r_1} \cos\theta \sin\theta \,\mathrm{d}\theta - \int_{\alpha_0}^{\alpha_1} \tau_{r\theta} \sin^2\theta \,\mathrm{d}\theta - \int_{\alpha_1}^{\alpha_2} \tau_{r\theta} \sin^2\theta \,\mathrm{d}\theta \\
&= (-2B\ln r_1 + A_1)(\sin^2\alpha_1 - \sin^2\alpha_0)/2 + 12(B - Y_1)[F_1(\alpha_1) - F_1(\alpha_0)] \\
&\quad + 3K_1[F_2(\alpha_1) - F_2(\alpha_0)] + (-2B\ln r_1 + A_2)(\sin^2\alpha_2 - \sin^2\alpha_1)/2 \\
&\quad + 12(B - Y_2)[F_1(\alpha_2) - F_1(\alpha_1)] + 3K_2[F_2(\alpha_2) - F_2(\alpha_1)] - 2(B - Y_1)[F_3(\alpha_1) - F_3(\alpha_0)] \\
&\quad - 2(B - Y_2)[F_3(\alpha_2) - F_3(\alpha_1)] + K_1(\cos\alpha_0 - \cos\alpha_1) + K_2(\cos\alpha_1 - \cos\alpha_2)
\end{aligned} \tag{19}$$

where the functions F_1, F_2 and F_3 are defined as:

$$\begin{aligned}
F_1(\theta) &= \int \ln\cos\frac{\theta}{2} \cos\theta \sin\theta \,\mathrm{d}\theta = \tfrac{1}{2}\sin^2\theta \ln\cos\frac{\theta}{2} + \tfrac{1}{2}\cos^4\frac{\theta}{2} - \cos^2\frac{\theta}{2} \\
F_2(\theta) &= \int \ln\tan\frac{\theta}{2} \cos\theta \sin\theta \,\mathrm{d}\theta = \tfrac{1}{2}\sin^2\theta \ln\tan\frac{\theta}{2} + \cos^2\frac{\theta}{2} \\
F_3(\theta) &= \int \tan\frac{\theta}{2} \sin^2\theta \,\mathrm{d}\theta = 2\sin^4\frac{\theta}{2}.
\end{aligned} \tag{20}$$

At this point, we have a system of five equations, (15)–(19), for five constants, K_1, K_2, B, A_1, A_2. Solving this system we get:

$$K_1 = \sin\alpha_0 \left[2(B - Y_1)\tan\frac{\alpha_0}{2} + \frac{m_0 Y_1}{\sqrt{3}} \right] \tag{21}$$

$$K_2 = \sin\alpha_2 \left[2(B - Y_2)\tan\frac{\alpha_2}{2} - \frac{m_2 Y_2}{\sqrt{3}} \right] \tag{22}$$

$$B = \frac{Y_2 \sin^2\frac{\alpha_2}{2} - Y_1 \sin^2\frac{\alpha_0}{2} + \frac{m_2 Y_2}{4\sqrt{3}}\sin\alpha_2 + \frac{m_0 Y_1}{4\sqrt{3}}\sin\alpha_0 + (Y_1 - Y_2)\sin^2\frac{\alpha_1}{2}}{\sin^2\frac{\alpha_2}{2} - \sin^2\frac{\alpha_0}{2}} = \bar{Y} + \Delta \tag{23}$$

$$A_1 = Y_1 + 12Y_1\left(\ln\cos\frac{\alpha_1}{2} + \sin^2\frac{\alpha_1}{2}\ln\tan\frac{\alpha_1}{2}\right) + C \tag{24}$$

$$A_2 = Y_2 + 12Y_2\left(\ln\cos\frac{\alpha_1}{2} + \sin^2\frac{\alpha_1}{2}\ln\tan\frac{\alpha_1}{2}\right) + C \tag{25}$$

with the mean yield stress being defined as

$$\bar{Y} = \frac{Y_2\left(\sin^2\frac{\alpha_2}{2} - \sin^2\frac{\alpha_1}{2}\right) + Y_1\left(\sin^2\frac{\alpha_1}{2} - \sin^2\frac{\alpha_0}{2}\right)}{\sin^2\frac{\alpha_2}{2} - \sin^2\frac{\alpha_0}{2}} \tag{26}$$

the friction contribution being determined by the parameter

$$\Delta = \frac{\frac{m_2 Y_2}{4\sqrt{3}}\sin\alpha_2 + \frac{m_0 Y_1}{4\sqrt{3}}\sin\alpha_0}{\sin^2\frac{\alpha_2}{2} - \sin^2\frac{\alpha_0}{2}} \tag{27}$$

and constant C in eqns (24) and (25) coming from (19) as

$$\begin{aligned} C = {} & \frac{-2}{\sin^2\alpha_2 - \sin^2\alpha_0}[(-2B\ln r_1 + \hat{A}_1)(\sin^2\alpha_1 - \sin^2\alpha_0) + 12(B - Y_1)[F_1(\alpha_1) \\ & - F_1(\alpha_0)] + 3K_1[F_2(\alpha_1) - F_2(\alpha_0)] + (-2B\ln r_1 + \hat{A}_2)(\sin^2\alpha_2 - \sin^2\alpha_1) \\ & + 12(B - Y_2)[F_1(\alpha_2) - F_1(\alpha_1)] + 3K_2[F_2(\alpha_2) - F_2(\alpha_1)] - 2(B - Y_1)[F_3(\alpha_1) - F_3(\alpha_0)] \\ & - 2(B - Y_2)[F_3(\alpha_2) - F_3(\alpha_1)] + K_1(\cos\alpha_0 - \cos\alpha_1) + K_2(\cos\alpha_1 - \cos\alpha_2)] \end{aligned} \tag{28}$$

where we denote:

$$\hat{A}_1 = A_1 - C \tag{29}$$

$$\hat{A}_2 = A_2 - C. \tag{30}$$

Therefore, the stress field for a bimetallic tube can be written as:

$$\begin{aligned} \sigma_{r_1} = {} & -2(\bar{Y} + \Delta)\ln r + 12Y_1\left(\ln\cos\frac{\alpha_1}{2} + \sin^2\frac{\alpha_1}{2}\ln\tan\frac{\alpha_1}{2}\right) + 12(\bar{Y} + \Delta - Y_1)\ln\cos\frac{\theta}{2} \\ & + 12(\bar{Y} + \Delta - Y_1)\sin^2\frac{\alpha_0}{2}\ln\tan\frac{\theta}{2} + \sqrt{3}m_0 Y_1\sin\alpha_0\ln\tan\frac{\theta}{2} + C + Y_1 \\ \sigma_{\theta_1} = {} & \sigma_{r_1} - Y_1 \\ \tau_{r\theta_1} = {} & 2(\bar{Y} + \Delta - Y_1)\tan\frac{\theta}{2} - \frac{4(\bar{Y} + \Delta - Y_1)\sin^2\frac{\alpha_0}{2} + \frac{m_0 Y_1\sin\alpha_0}{\sqrt{3}}}{\sin\theta} \end{aligned} \tag{31}$$

for material 1, and

$$\sigma_{r_2} = -2(\bar{Y}+\Delta)\ln r + 12Y_2\left(\ln\cos\frac{\alpha_1}{2} + \sin^2\frac{\alpha_1}{2}\ln\tan\frac{\alpha_1}{2}\right) + 12(\bar{Y}+\Delta-Y_2)\ln\cos\frac{\theta}{2}$$

$$+12(\bar{Y}+\Delta-Y_2)\sin^2\frac{\alpha_2}{2}\ln\tan\frac{\theta}{2} - \sqrt{3}m_2 Y_2 \sin\alpha_2 \ln\tan\frac{\theta}{2} + C + Y_2$$

$$\sigma_{\theta_2} = \sigma_{r_2} - Y_2$$

$$\tau_{r\theta_2} = 2(\bar{Y}+\Delta-Y_2)\tan\frac{\theta}{2} - \frac{4(\bar{Y}+\Delta-Y_2)\sin^2\frac{\alpha_2}{2} - \frac{m_2 Y_2 \sin\alpha_2}{\sqrt{3}}}{\sin\theta} \tag{32}$$

for material 2. For small die angles, (31) and (32) reduce to the solution given by Durban (1984).

Finally, the total force required for the process may be estimated through the integration of forces in the axial direction, x: $F = \int \sigma_x \, dS$, where $dS = 2\pi r_0^2 \sin\theta \, d\theta$ is a surface element in spherical coordinates, and the axial stress is $\sigma_x = \sigma_r \cos\theta - \tau_{r\theta}\sin\theta$. From this calculation, it is obtained:

$$F = 2\pi r_0^2 \int_{\alpha_0}^{\alpha_1} \sigma_r^{(1)}\Big|_{r_0} \cos\theta\sin\theta\,d\theta + \int_{\alpha_1}^{\alpha_2} \sigma_r^{(2)}\Big|_{r_0} \cos\theta\sin\theta\,d\theta - \int_{\alpha_0}^{\alpha_1} \tau_{r\theta}\sin^2\theta\,d\theta - \int_{\alpha_1}^{\alpha_2} \tau_{r\theta}\sin^2\theta\,d\theta$$

$$= 2\pi r_0^2\left(-B\ln\frac{r_0}{r_1}\right)(\sin^2\alpha_2 - \sin^2\alpha_0). \tag{33}$$

4. RESULTS

In this section, eqns (31) and (32) will be applied to different geometries, materials and extrusion conditions. To illustrate the behaviour of the stress solution, let us first consider a particular case for each of the two possible locations of the corrosion resistant alloy (C.R.A.), acting as an inner or outer layer. Data in both cases are taken from an actual process used in Tubacex (Llodio, Spain). In the notation, we refer to σ_r, σ_θ and $\tau_{r\theta}$ as the radial, normal and shear stress, respectively.

4.1. *Application to Inconel* 625 *and AISI* 4130

4.1.1. *Inner C.R.A. location.* Let us start with the case of an inner C.R.A. location. The initial tube exhibits an inner/outer thickness ratio of 1/5 and an inner/outer yield stress ratio of 2.2. The remaining dimensions and parameters are included in Table 1.

The application of eqns (31) and (32) provide the stress distributions plotted in Fig. 2, after being normalized with the yield stress of the base steel (AISI 4130). Figure 2a shows the radial stress at $\theta = \alpha_0$, α_1 and α_2, as a function of the radial coordinate, and Fig. 2b displays the radial stress at $r = r_0$ and r_1 (i.e. the entry and exit surfaces, respectively), as a function of the angular coordinate, θ. According to the von Mises model for a rigid-plastic material, a discontinuity of value $Y_1 - Y_2$ across the interface is obtained. A small dependence on the θ angle can also be noticed both in Figs 2a and 2b. The highest values of the radial stress occur in the harder material. Furthermore, these values increase on

Table 1. Normalized reference values for both locations of the C.R.A. layer [R_0 and R_f stand for the outer radius at the entry and exit sections, respectively; R_1 for the initial interface radius; R_m for the mandrel radius; m_0 and m_2 for the friction coefficient with the mandrel and die, respectively, and α_0, α_1, α_2 for the mandrel, interface and die angle, respectively]

Case	Y_1/Y_2	α_0	α_1	α_2	R_1/R_0	R_m/R_0	R_f/R_0	m_0	m_2
Inner C.R.A.	2.2	9.15°	12.5°	30°	0.436	0.32	0.73	0.1	0.15
Outer C.R.A.	1/2.2	9.15°	24.3°	30°	0.884	0.32	0.73	0.1	0.15

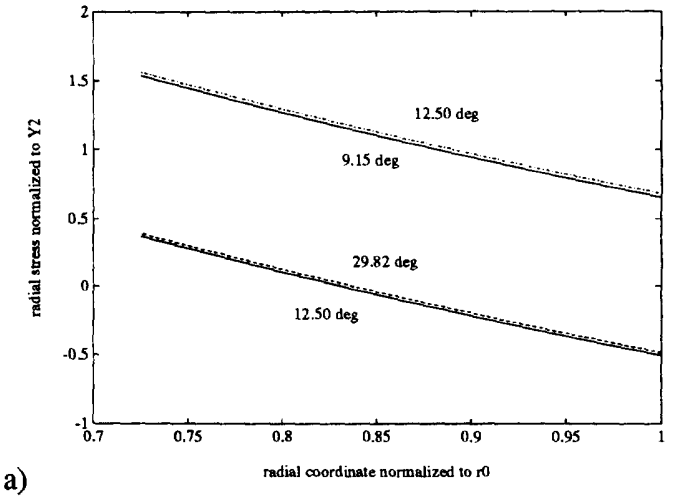

a)

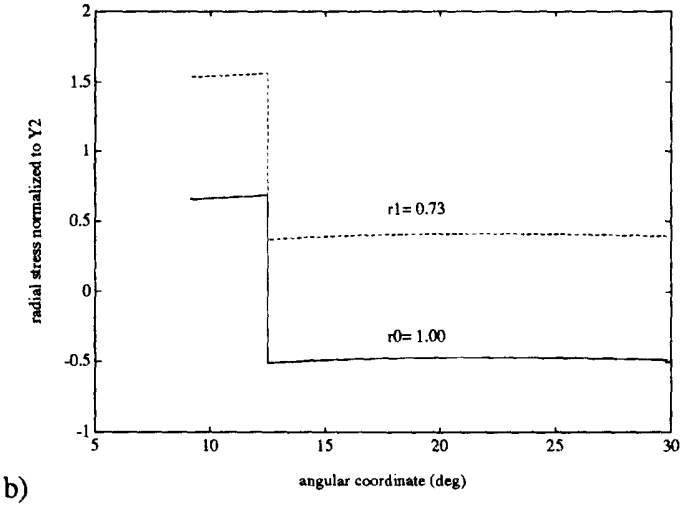

b)

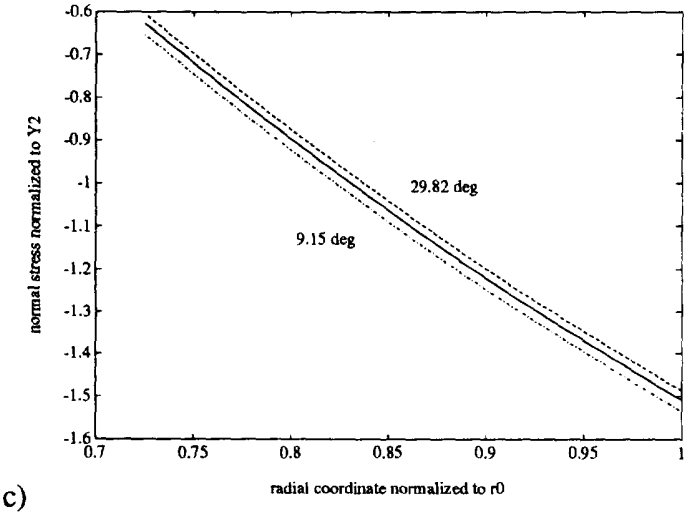

c)

Fig. 2. Normalized stresses for the inner C.R.A. case: (a) radial stress at α_0, α_1 and α_2, (b) radial stress at r_0 and r_1, (c) normal stress at α_0, α_1 and α_2, (d) normal stress at r_0 and r_1, (e) shear stress. [$\alpha_0 = 9.15°$, $\alpha_1 = 12.5°$, $\alpha_2 = 30°$, $r_0 = 0.346$ m and $r_1 = 0.251$ m.] (*Continued opposite.*)

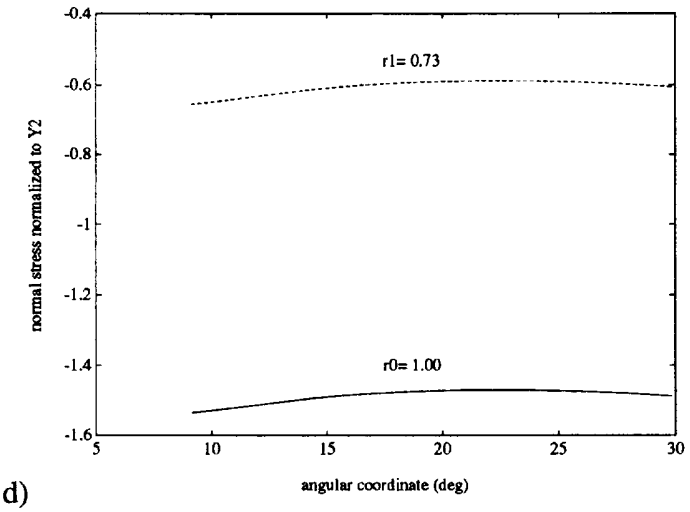

d)

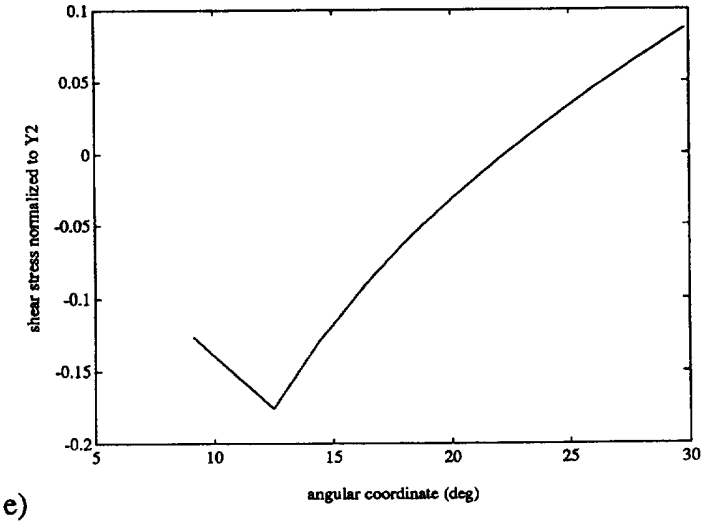

e)

Fig. 2—(*Continued.*)

approaching the die exit. The sign of the radial stress in the outer material changes during the process, remaining positive at the exit. The inner material, however, remains always tractive. These residual stresses prove to be important wherever positive, because they could induce some decohesion in the final product.

The normal stress is plotted in Figs 2c–d for the same values of θ and r as in Figs 2a–b. It can be seen, from Fig. 2c, that this stress component is continuous across the interface and takes negative values in both materials. Figure 2d shows that the influence of θ is also negligible. The module of this stress component in the inner layer (the harder material) is higher than in the outer layer and decreases upon approaching the exit.

Finally, Fig. 2e shows the shear stress as a function of θ. According to (12c), this stress component does not depend on the radial coordinate. Figure 2e also shows that the maximum absolute value is attained at the interface (as also pointed out by Pawelski and Rasp, 1978). The shear stress is negative at the interface and diminishes in module at farther locations. The outer material being thicker, the sign even changes within this material. The order of magnitude of the shear stress is a unit lower than that of the two other stresses.

4.1.2. *Outer C.R.A. location.* Consider now the opposite situation, with the C.R.A. layer placed outerly (i.e., a combination AISI 4130/Inconel 625). In this case, the inner/outer

thickness ratio of the tube is 5 and the inner/outer yield stress ratio is 1/2.2. Other parameters can be found in Table 1.

Similarly to Fig. 2, the stress distributions are depicted in Fig. 3. They are again normalized with the yield stress of the base steel. As shown in Figs 3a–b, the radial stresses are higher in the C.R.A. layer than in the other, as occurred in the case with an inner C.R.A. (although the maximum value is now a little higher). Likewise, from Figs 3c–d normal stresses in the C.R.A. material are obtained higher in module than in the base steel, as in Figs 2c–d. Finally, the shear stress shown in Fig. 3e has an opposite sign in the harder material and its magnitude is almost doubled, as compared to Fig. 2e. Note that the stress levels in Fig. 3 are higher than in Fig. 2, because the material interface flows nearer the die.

4.2. *Influence of the extrusion parameters*

In this section, we proceed with a systematic analysis of the influence of the different parameters involved in eqns (31) and (32). As before, the two cases (with outer and inner C.R.A.) will be clearly distinguished. The reference values for the two locations are the same given in Table 1.

To establish an appropriate comparison among the different cases, some characteristic values are selected. According to Figs 2 and 3, and as experience confirms, the interfacial point at the die exit provides the most dangerous stress state. Therefore, stresses at this location are selected. Note that two sets of values can be obtained: one in each material. These values will again be normalized with respect to the yield stress of the common steel alloy.

4.2.1. *Inner C.R.A. location.* The results of the stress components for an inner C.R.A. location are plotted in Figs 4a–f. In this case, the stresses are computed in the inner interface element, which provides higher levels than the outer one.

Figure 4a shows the influence of the yield stress ratio (Y_1/Y_2). It can be noticed that as this ratio increases all the stresses increase in module, because of the higher yield stress of the harder material and the more critical heterogeneity at the interface. The radial stress reaches the highest values and most important variation. Compared to the remaining parameters, the yield stress ratio becomes one of the most influential variables.

In Fig. 4b, the effect of the die angle is illustrated. With higher angles, the shear and normal stresses increase in module, while the radial stress diminishes. The explanation of this behaviour is that a higher die angle makes the stresses more compressive (towards negative values).

The effect of the interface radius is shown in Fig. 4c. An increase in this magnitude produces similar effects as the increase in the die angle, i.e., the negative stress components (especially the normal stress) increase in module and the radial stress becomes less positive. Two reasons could be given to understand this behaviour. Firstly, the stresses are more compressive when the interface approaches more the die. And besides, a higher interface radius implies that the thickness of the harder material (inner location) increases.

The results of the influence of the mandrel size are shown in Fig. 4d. The effect of an increase in this parameter is the opposite to that of an increase in the interface radius, because of using larger mandrels, the thickness of the inner harder material decreases. In particular, we obtain higher radial stresses, lower (in module) normal stresses and almost identical shear stresses.

It has been verified that the final size of the tube (or, equivalently, the extrusion ratio) has no influence on the stress representative levels. Although this result could be surprising, it derives naturally from the consideration of a spherical radial flow and the vanishing of the resulting axial stress at the die exit section (see (19)).

The effects of the friction coefficients (m_0 and m_2) are plotted in Figs 4e and f, respectively. The friction with the mandrel slows down the flow of the inner harder material. For this reason, Fig. 4e shows that the positive radial stress increases and the shear stress becomes more negative as m_0 increases. There is also a tractive effect on the normal component. On the other hand, Fig. 4f shows that the friction with the die makes the radial stress increase, since it involves a hindrance to the flow. On the other hand, the shear stress

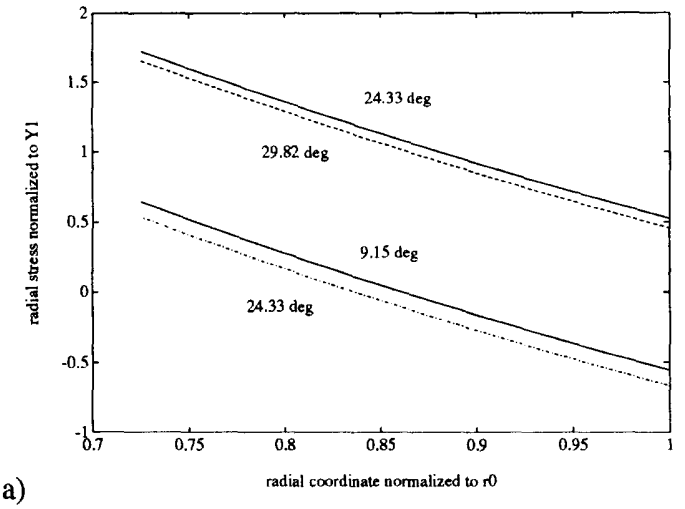

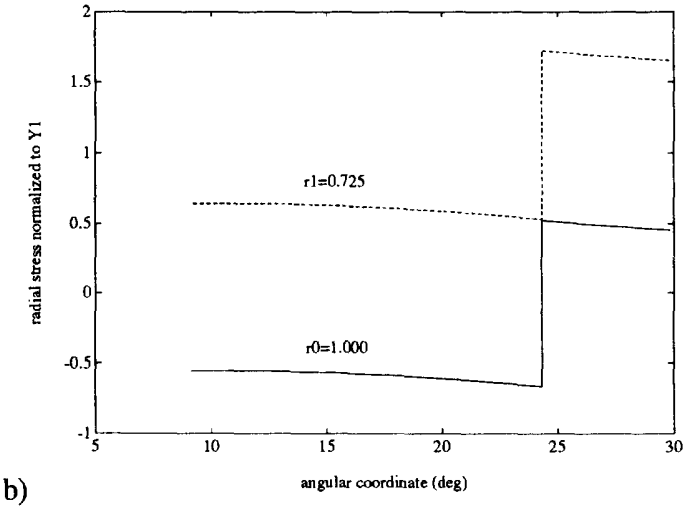

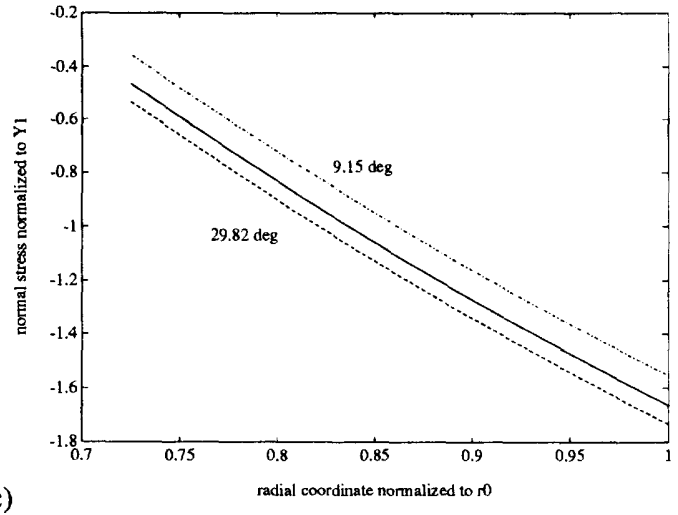

Fig. 3. Normalized stresses for the outer C.R.A. case: (a) radial stress at α_0, α_1 and α_2, (b) radial stress at r_0 and r_1, (c) normal stress at α_0, α_1 and α_2, (d) normal stress at r_0 and r_1, (e) shear stress. [$\alpha_0 = 9.15°$, $\alpha_1 = 24.3°$, $\alpha_2 = 30°$, $r_0 = 0.346$ m and $r_1 = 0.251$ m.] (*Continued overleaf.*)

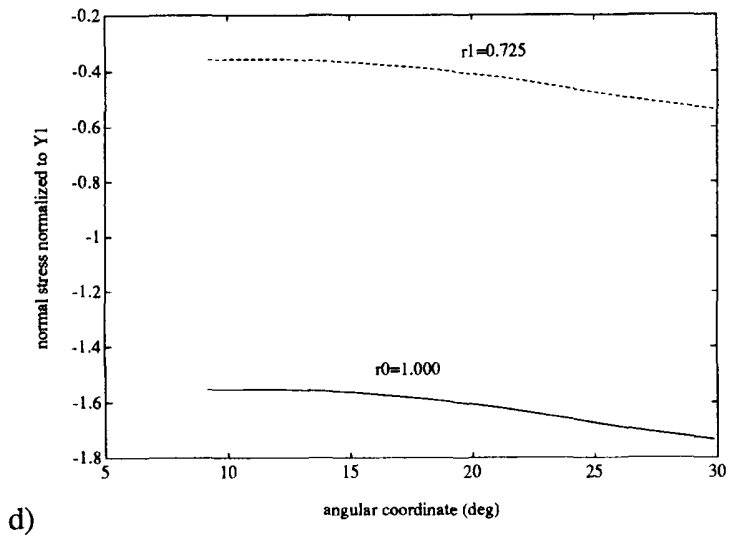

d)

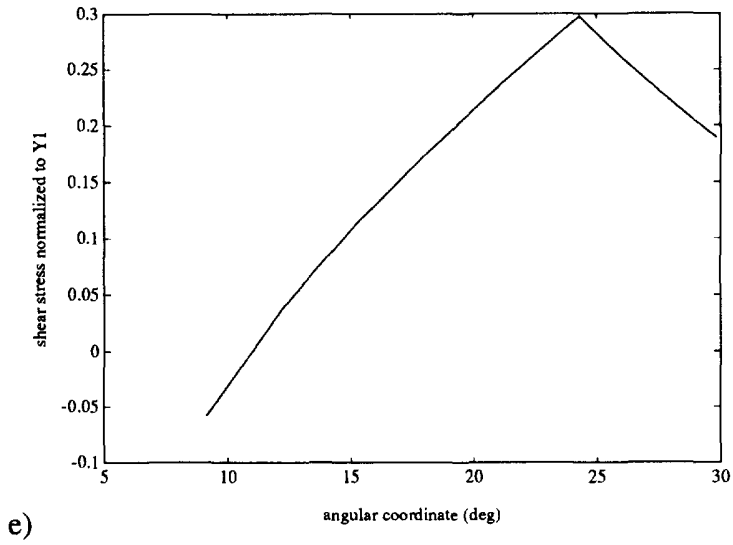

e)

Fig. 3—(*Continued.*)

becomes less negative, although this influence is small due to the farther distance from the die. A tractive effect of an increasing m_2 coefficient is also noticeable on the normal stress.

4.2.2. *Outer C.R.A. location.* In the case of a tube with an outer C.R.A. location, stresses are selected at the interface point in the outer material. The results are plotted in Figs 5a–f. As the outer layer is now extruded with more difficulty, shear stresses assume positive values in the C.R.A. and a change of sign takes place in the base steel. Normal stresses remain negative.

The influence of the yield stress ratio Y_1/Y_2 is shown in Fig. 5a. As expected, the shear and radial stresses increase with that ratio, due to a higher C.R.A. yield stress combined with a stronger discrepancy in the plastic flow. The normal stress slightly diminishes in module as the yield stress ratio increases.

Figure 5b illustrates the effect of the die angle. At higher angles, the radial and normal stresses become more compressive (as in Fig. 4b) and the shear stress increases its value. This latter effect is attributed to the fact that high die angles involve more flow disturbance in the outer layer, thus making the shear component at the interface increase.

The influence of the interface radius, shown in Fig. 5c, differs from the inner C.R.A. case. The normal stress diminishes in module with the increase in the interface radius,

because of the correlative decrease in the thickness of the outer layer (the C.R.A.). On the other hand, as the interface approaches the die, the shear stress slightly increases and the radial stress also increases due to the more favourable geometric conditions for the inner

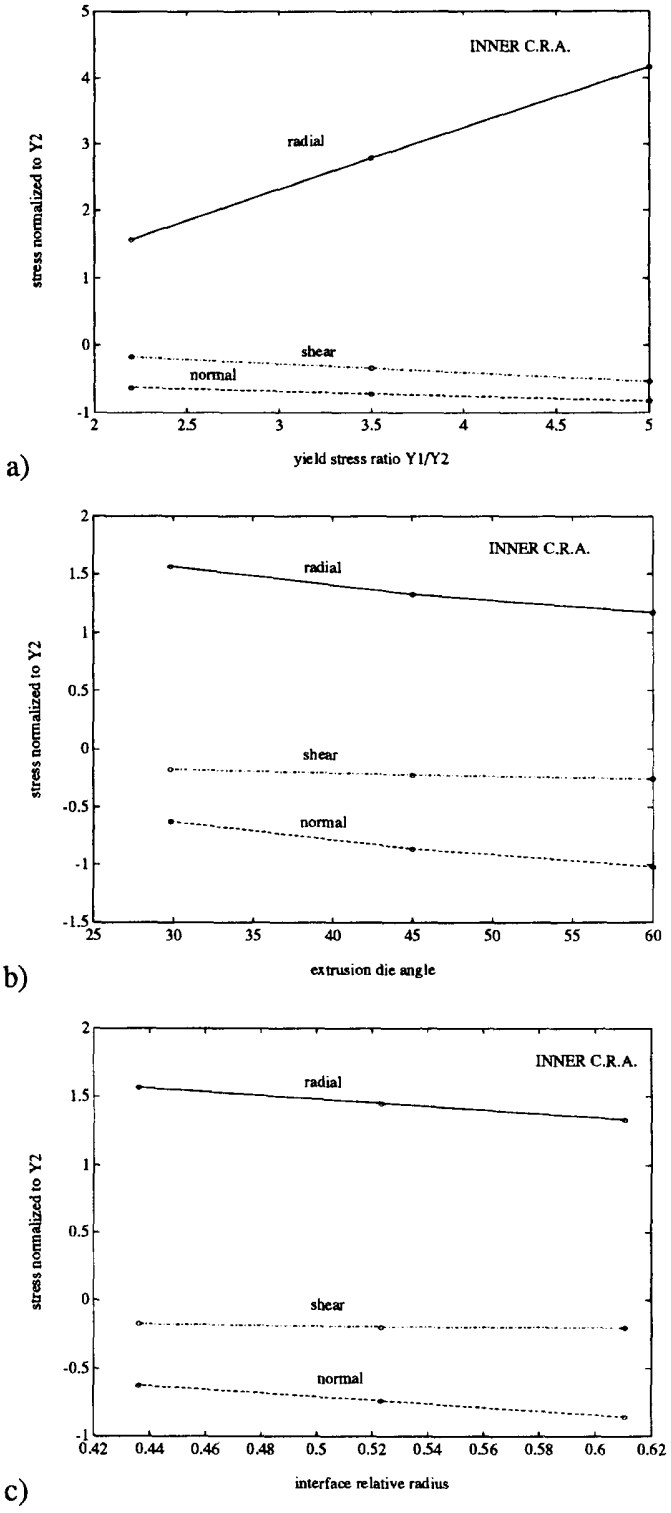

Fig. 4. Influence of the extrusion parameters on the stress levels at the exit interfacial point for the inner C.R.A. case: (a) yield stress ratio, (b) extrusion die angle, (c) interface relative radius, (d) mandrel relative radius, (e) friction coefficient with the mandrel, (f) friction coefficient with the die.

(*Continued overleaf.*)

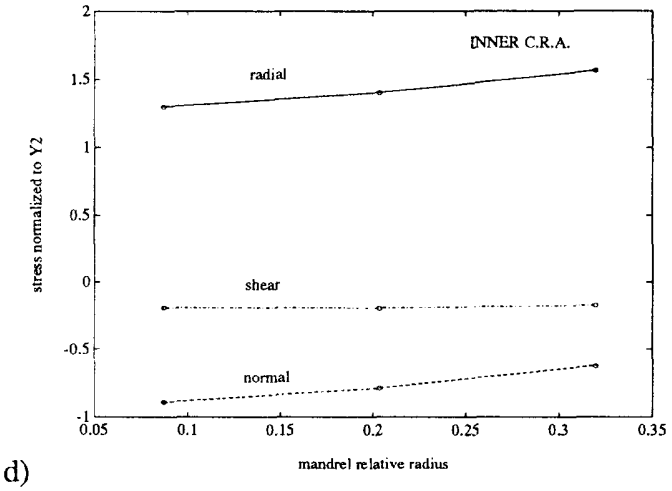

d)

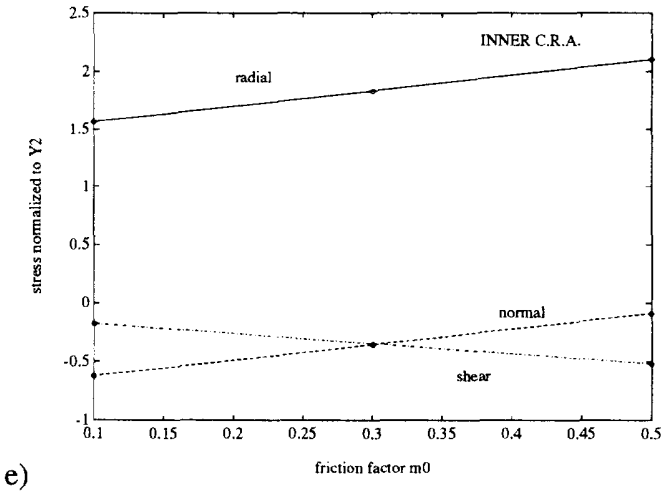

e)

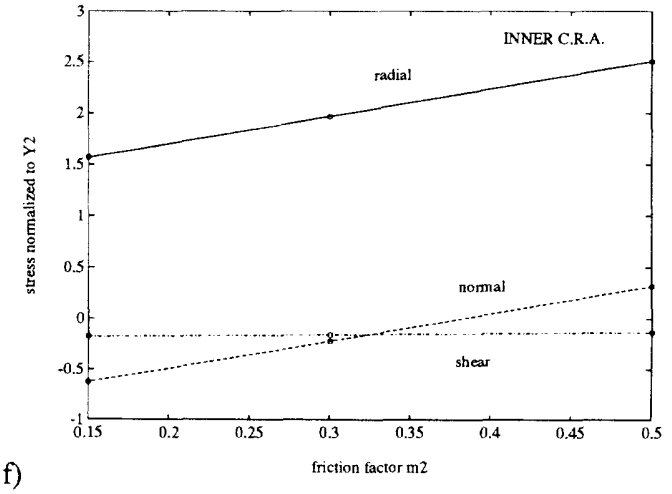

f)

Fig. 4—(*Continued.*)

material to flow and, consequently, the more pronounced effect of the inner material on the outer one. The tractive effect of the inner material affects the variation of both the normal and radial stress.

By assuming several mandrel sizes, Fig. 5d is obtained. It can be seen that on increasing the relative size of the mandrel only small stress variations are derived: a lower-in-module normal stress, a lower shear stress and a higher radial stress. Moreover, these variations

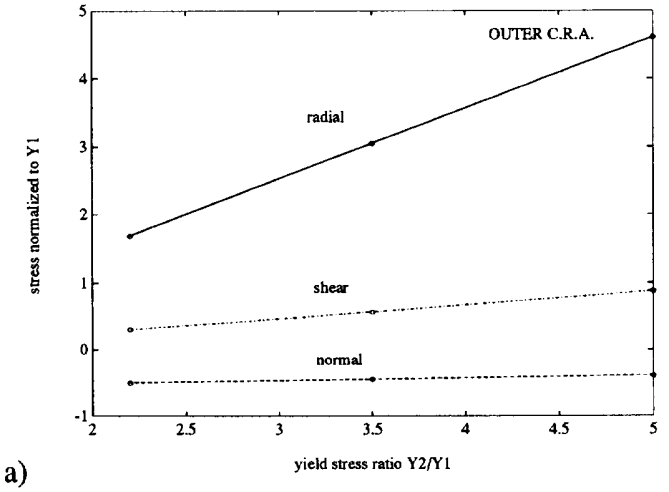

a)

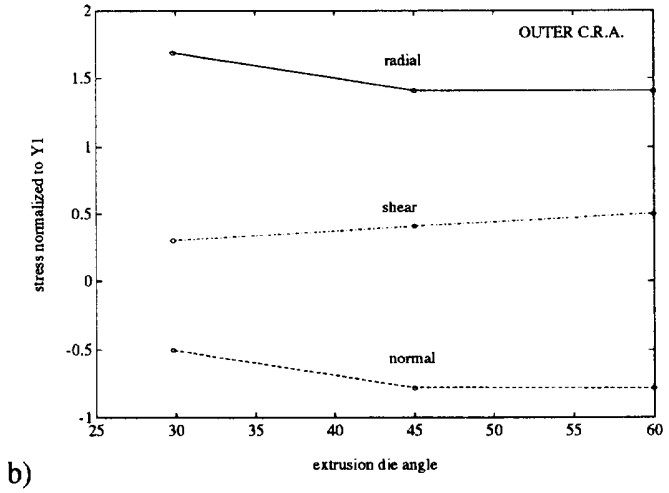

b)

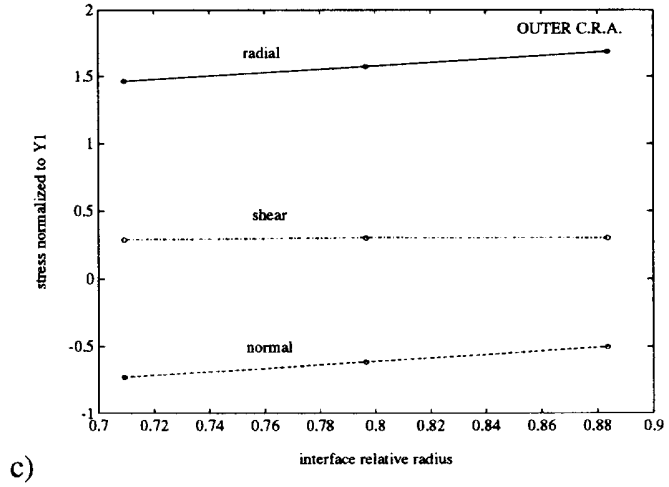

c)

Fig. 5. Influence of the extrusion parameters on the stress levels at the exit interfacial point for the outer C.R.A. case: (a) yield stress ratio, (b) extrusion die angle, (c) interface relative radius, (d) mandrel relative radius, (e) friction coefficient with the mandrel, (f) friction coefficient with the die.

(*Continued overleaf.*)

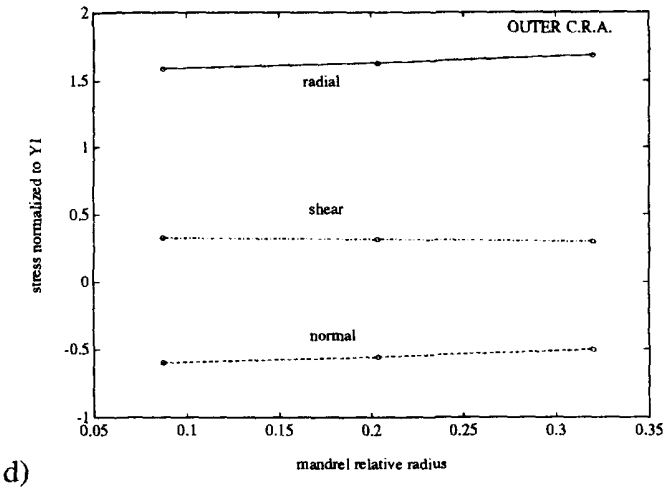

d)

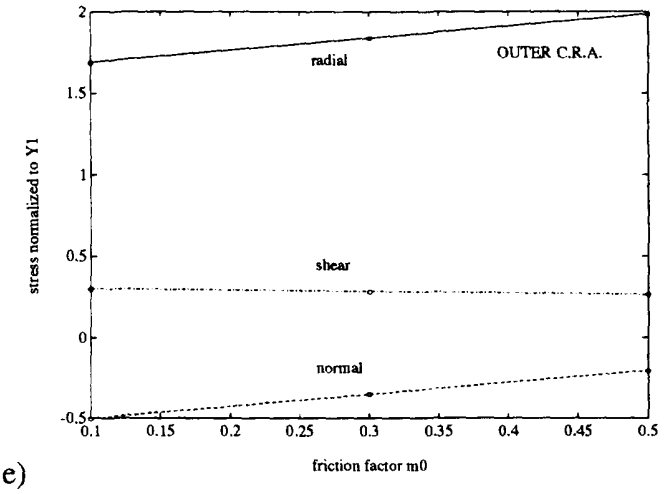

e)

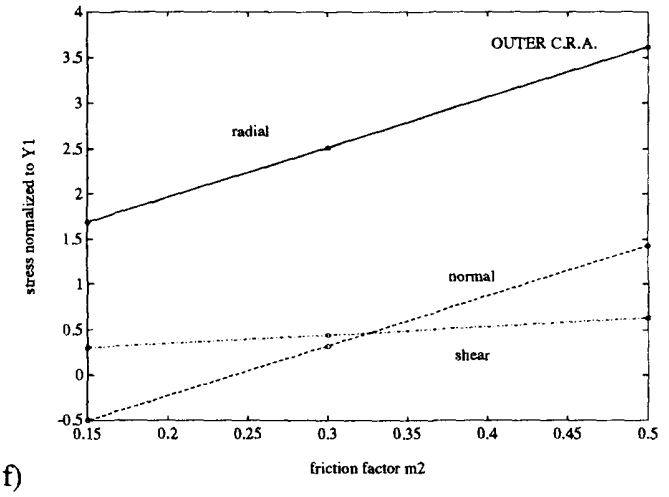

f)

Fig. 5—(*Continued.*)

are very similar to those in Fig. 5c. Since the increase in the mandrel size implies the decrease in the inner material thickness, the effect of the yield discrepancy between the layers turns out to be reduced. This leads to a decrease in the normal and shear stresses at the interface. The radial stress, however, increases because the inner yielding is facilitated by a larger mandrel.

Table 2. Evaluation of the void growth parameter, f, on varying different extrusion parameters for an inner C.R.A. location

			Inner C.R.A.				
Y_1/Y_2	f	R_f/R_0	f	m_0	f	m_2	f
2.2	0.128	0.553	0.074	0.1	0.128	0.15	0.128
3.5	0.52	0.64	0.095	0.3	0.45	0.3	0.92
5	0.87	0.727	0.128	0.5	0.75	0.5	1.57

Finally, the variations in stress with the friction coefficients m_0 and m_2 are plotted in Figs 5e and f, respectively. Similarly to the inner C.R.A. case, an increase in both friction coefficients involves a tractive effect on the normal stress and a higher radial component (because this component opposes the flow). However, the shear stress, being now positive (i.e., in the sense of the flow), decreases slightly with the mandrel friction and increases with the die friction. As shown in Fig. 5e, the effects of an increase in the mandrel friction are similar to and more pronounced than those of an increase in the mandrel size. The flow of the softer material is impeded by the mandrel friction, giving rise to lower shear stresses and also lower in module normal stresses at the interface. On the other hand, an increase in the die friction (Fig. 5f) prevents the flow of the outer, leading to an increase in the shear and radial stresses. For coefficients higher than 0.25, it is also noticed in Fig. 5f that there is a change of sign in the normal stress, due to the proximity of the interface to the die.

5. DUCTILE FAILURE

Up to now stress fields have been derived and the influence of the extrusion parameters on the maximum stress at the interface has been stated. In this section, a ductile failure criterium will be established so as to assess the most critical conditions and variables in the process.

Let the *void growth parameter* f be defined as:

$$f = \int_0^{\bar{\varepsilon}} \exp\left(1.5\frac{\sigma_h}{\bar{\sigma}}\right)\overline{\mathrm{d}\varepsilon}, \quad \sigma_h > 0 \tag{34}$$

where $\bar{\sigma}$ and $\bar{\varepsilon}$ are the equivalent plastic stress and strain, respectively, and σ_h is the hydrostatic stress. According to (34), this parameter represents an accumulated plastic strain corrected by the hydrostatic stress and will be considered here as an indication of ductile failure. It is based on a factor deduced by Rice and Tracey (1969). The fracture condition will locally be fulfilled wherever a critical value of f is attained.

The results from the evaluation of the parameter f, normalized with respect to the uniform equivalent strain ($\ln A_0/A_f$, where A_0 and A_f are respectively the initial and final cross section of the tube), are included in Tables 2 and 3. In the case of an inner C.R.A. location (Table 2), the most important variations take place for the friction coefficients, m_0 and m_2. On using high friction coefficients, the normal stress at the exit point of the interface decreases considerably, even assuming positive values. Another relevant variable is the yield stress ratio, Y_1/Y_2, which gives rise to variations similar to those of the friction coefficients. Finally, on decreasing the final radius (i.e., increasing the extrusion ratio), the factor f

Table 3. Evaluation of the void growth parameter, f, on varying different extrusion parameters for an outer C.R.A. location.

					Outer C.R.A.						
Y_2/Y_1	f	R_1/R_0	f	R_m/R_0	f	R_f/R_0	f	m_0	f	m_2	f
2.2	0.202	0.708	0.004	0.085	0.12	0.553	0.112	0.1	0.202	0.15	0.202
3.5	0.49	0.795	0.092	0.205	0.155	0.64	0.149	0.3	0.343	0.3	1.1
5	0.69	0.882	0.202	0.32	0.202	0.727	0.202	0.5	0.48	0.5	2.15

assumes lower values. Although the absolute value of f does not change, as commented in Section 4, its normalized value diminishes since the total uniform strain increases at higher extrusion ratios. Notwithstanding, the values obtained are very small.

Other parameters such as the die angle, the interface radius and the mandrel radius are not included in Table 2. In the first place, on increasing the die angle (above 30°), negative hydrostatic stresses are obtained in the selected point. Therefore, there will be no tendency to void formation under these conditions. On the other hand, the same behaviour is also encountered on increasing the interface radius or on decreasing the mandrel radius. In both cases, the C.R.A. thickness increases and, as mentioned before, more compressive stresses are attained, the hydrostatic stress becoming negative along the interface. Accordingly, eqn (34) cannot be evaluated for these three parameters.

The results for the outer location of the C.R.A. layer are included in Table 3. Again, the friction coefficients (especially with the die) provide the largest variations in the factor f. The yield stress ratio also gives rise to important increments in the void growth parameter.

On the other hand, on increasing the interface radius or the mandrel radius, an increase in the factor f can be noticed, since more compressive stresses are then obtained. The final radius affects the parameter f very little: higher extrusion ratios give rise to lower factors. Finally, the die angle is not included in Table 3, for the same reason commented before for Table 2.

6. DISCUSSION

A brief discussion on the method and results is presented in this section. In the first place, it should be noted that the analysis leads only to a first approach to the real process. The accuracy of the results is strongly conditioned by simplified assumptions on the flow. Nevertheless, the method proves to be quick and easy, and allows an efficient analysis of the repercussion of the many parameters involved in the process.

The bonding along the interface does not play any role in the method. Therefore, the solution would be valid for a real flow with perfect bonding, where the velocity continuity is imposed along the material interface.

The piston force computed through eqn (33) provides a value very similar to Durban's and of the same order as Blazynski and Townley's. It differs, however, from the actual industrial process because it does not take into account the discontinuities at the entry and exit sections, and other possible redundant contributions.

A comparison between the present results and finite element calculations (Alcaraz, 1993) under similar conditions shows that stress values of the same order are obtained (for both locations of the C.R.A.). The main difference takes place in the shear stress distribution. Here this component was shown to be independent on the radial coordinate. However, by FE results some dependency is found, showing an evolution from negative values at the entry to positive values at the exit. Notwithstanding this fact, the magnitude is the same order likewise. The sign and values of this shear stress along the contact zones (with mandrel and die) have also been checked. Finally, the qualitative incidence of some of the extrusion variables (the yield stress ratio, the die angle and the thickness ratio) can also been verified by FE results in Alcaraz (1993).

7. CONCLUSIONS

An analytical approach of the stress field in the extrusion of bimetallic tubes has been performed and the influence of some relevant parameters of the process has been discussed.

The radial and normal stress components show very small dependence on the angular coordinate, which means a quasi-uniform flow. Moreover, the shear stress component does not depend on the radial coordinate (as a result of the spherical radial flow assumed in the analysis).

For an inner location of the harder material, the stress plots show that the radial stress is positive and the shear stress negative in the harder material. The signs change for the

opposite location. Normal stresses are negative in all cases and show a decreasing trend in module on approaching the die exit.

A comparison in the stress levels at the exit interfacial point shows that higher stresses are obtained with higher yield stress ratios and die angles, and when the proportion of the harder material increases at an inner location. However, lower shear and radial stresses are derived with an outer location of the harder material.

The stress values obtained at the interface are also used to assess a factor indicative of the ductile failure of the tube. It is concluded that the most influential parameters seem to be the yield stress ratio and the friction (especially with the die). Higher values of the defined factor are also obtained when the thickness of the harder layer decreases. Increasing the die angle, on the other hand, propitiates more compressive stresses and thus helps to prevent the void growth ductile failure.

REFERENCES

Alcaraz, J. L. (1993). Analysis of the deformation and failure conditions in the extrusion of bimetallic tubes. Ph. D. Dissertation, San Sebastián, Spain.

Atkins, A. G. and Weinstein, A. S. (1970). The deformation of sandwich materials. *Int. J. Mech. Sci.* **12,** 641–657.

Avitzur, B., Wu, R., Talbert, S. and Chou, Y. T. (1982). Criterion for the prevention of core fracture during extrusion of bimetal rods. *ASME J. Engng Ind.* **104,** 293–304.

Avitzur, B., Wu, R., Talbert, S. and Chou, Y. T. (1986). Criterion for the prevention of sleeve fracture during extrusion of bimetal rods. *ASME J. Engng Ind.* **108,** 205–212.

Blazynski, T. Z. and Townley, S. (1978). The methods of analysis of the process of plug drawing of bimetallic tubing applied to implosively welded composites. *Int. J. Mech. Sci.* **20,** 785–797.

Durban, D. (1984). Drawing and extrusion of composite sheets, wires and tubes. *Int. J. Solids Struct.* **20,** 649–666.

Hartley, C. S. (1973). Upper bound analysis of extrusion of axisymmetric, piecewise homogeneous tubes. *Int. J. Mech. Sci.* **15,** 651–663.

Nagy, A. T. (1985). Drawing of a material consisting of a hard core and a soft sleeve. *J. Mech. Work. Tech.* **12,** 67–77.

Osakada, K., Limb, M. and Mellor, P. B. (1973). Hydrostatic extrusion of composite rods with hard cores. *Int. J. Mech. Sci.* **15,** 291–307.

Pawelski, O. and Rasp, W. (1979). Stresses and strains in deformation of clad metals. In *Metal Forming Plasticity*. (eds H. Lippmann *et al.*), pp. 363–377. Springer-Verlag, Berlin.

Rice, J. R. and Tracey, D. M. (1969). On the ductile enlargement of voids in triaxial stress fields. *J. Mech. Phys. Solids* **17,** 201–217.

Shield, R. T. (1955). Plastic flow in a converging conical channel. *J. Mech. Phys. Solids* **3,** 246–258.

Taheri, A. K. (1993). Analytical study of drawing of non-bonded trimetallic strips. *Int. J. Mach. Tools Manuf.* **33,** 71–88.

Tokuno, H. and Ikeda, K. (1991). Analysis of deformation in extrusion of composite rods. *J. Mat. Proc. Tech.* **26,** 323–335.

Yang, D. Y., Kim, Y. G. and Lee, C. M. (1991). An upper-bound solution for axisymmetric extrusion of composite rods through curved dies. *Int. J. Mach. Tools Manuf.* **31,** 565–575.